Ang, King, Lam, Lao, Yang
EE – 198B
May 25, 2006
Final Report
Running Head: PHOTOVOLTAIC CELLS

Optical Electric Guitar Pickup

Department of Electrical Engineering

San Jose State University

Abstract

This report illustrated the designs and specifications of an optical electric guitar pickup. The optical pickup detects signals from the strings and converts the signals into audio signals. The project was divided into three subsystems: detection, amplification, and summation. The detection stage consisted of six optical transmitters and three photodiodes all with the central wavelength of 940nm. The signal was then sent to the amplification stage, where we amplified the signals and adjusted for the DC offset of the signals Finally, the signals were combined at the summing stage before being sent to the quarter jack. This report also included an analysis of why we changed the design from the reflection method to the transmission method.

Introduction

Most musicians pursue quality sounds from their instruments, but the sounds that are produced are always distorted by noise. For an electric guitar, noise may be generated by the surrounding electronics, such as fluorescent lamps or transformers from other electrical and magnetic equipments. To minimize this problem, we came up with the design for an optical pickup for an electric guitar using infrared light sources and detectors. Most optical pickup system employs an enclosed case for the pickup to shield the pickup from the surrounding light sources, since a typical optical pickup uses visible light to detect the vibrations of the string. A typical optical pickup also filters potential undesirable light signals coming from around the stage, thus minimizing the noise that will be produced when it is used on stage. By filtering the signal, the pickup may also eliminate some of the higher order harmonics from the strings, which is an important component of the audio signal. By choosing to use infrared light sources for our project, we will be able to lower the noise generated from the surrounding light sources. In addition, the humming noises that most magnetic pickup produces will be greatly reduced by the optical pickup as we eliminate most of the noise resulting from the surrounding magnetic sources.

The design for our optical electric guitar pickup has four specifications. First, the pickup will produce an output signal within the frequency range of 20 Hz to 20kHz, which is the limit of perception of the human hear. The second specification requires the pickup to be able to detect the different frequencies from the strings, including the higher harmonics. The third specification is to have a low noise output and an amplified signal. In other words, the pickup has to produce an undistorted and usable signal. Lastly and the most important specification of all is not to change or modify the techniques of playing a guitar.

This optical pickup is consisted of three separate stages. The first stage is to extract the analog signals from the optical signals. The second stage is to amplify the detected signal using variable gain. The amplification stage will amplify the detected signal and adjust for the dc offset resulting from each sensor. The last stage of the project is to combine the signals from the three sensors using a summing amplifier in the non-inverting configuration. Finally, the output of the summing amplifier is fed into the audio amplifier through the quarter-jack.

Procedure:

In this project, we will try to extract the audio signal from the vibrating strings of an electric guitar by means of optical transmission. In the original design of the project, we proposed to use a reflection method where we place an array of infrared LED into the body of the guitar and point the array in the direction of the strings. Theoretically, the infrared wave will then reflect off the strings and into the sensors that we placed in the body of the guitar. In the original design, we would expect the reflected signals to be amplitude modulated and we would need to place a low pass filter at the output in order to extract the modulated signal.

Before we attempted to implement the reflection method, we experimented with the project by using a laser pointer and a photo-resistor. We pointed the laser pointer directly at the photo-resistor and

place the low E string in between the laser pointer and the photo-resistor. We then connected the leads of the photo-resistor to the oscilloscope to see if we can detect the vibration of the string. With the laser pointer and photo-resistor setup, we were able to see the changes on the oscilloscope as we move the laser pointer around the photo-resistor. We then tried to detect the motion of the string by placing the low E string between the laser pointer and the photo-resistor. We were unable to detect any signal using the oscilloscope as the string vibrated between the laser pointer and the photo-resistor.

We then attempted to reflect the infrared signal off of the strings by placing both the infrared LED array and the sensors in the body of the guitar. We varied the incident angles of the LEDs array while attempting the reflection method, but we were once again unable to extract any signal from the reflection of the strings with the different angles that we tried. We were able to observe the background infrared noise due to the fluorescent light to be around 50mV and we were able to eliminate this by covering the entire apparatus with a box. We concluded that if we only use the infrared LED array and the photodiodes, we would not be able to obtain any usable signals due to the lack of reflections and the excess infrared noise that surrounds us.

We then attempted to reflect the signals off of more reflective materials, such as aluminum. We tested our hypothesis by reflecting the LED array off of a piece of aluminum foil and place the strings in between the LED array and the aluminum foil. While the sensor was able to detect the general movement from the reflection due to the movements of the LED array, we were still unable to detect any usable signal from the vibration of the strings. With additional adjustments, (i.e. coating the strings with reflective paint, focusing the light sources, and using polarized lenses as optical filters), we may be able to achieve desirable results. As we learn later from the transmission method, the ratio of the exposed area of the sensor to the width of the string will also greatly affect our sensors abilities to detect the vibrations through the reflections.

Finally, we changed our design from the reflection method to the transmission method, where we placed the LED array outside of the body of the guitar and directly on top of the sensors. Using the transmission method, we were able to trace the vibrating motion of the strings by detecting the shadows of the strings with the photodiodes. In order to detect usable signals from the three sensors, we needed to vary the area of sensors that are exposed to the vibrating strings. For the wider strings (low E and A), the corresponding sensor needed to have larger exposed area than the sensor used to detect the narrower strings (B and high E). While we need to keep the ratio of the strings and the exposed area on the sensors constant for all three sensors and all six strings, we also need to keep the exposed sensor areas as low as possible due to the high DC offset the sensor introduces to the circuit.

Schematics and Simulation Analysis:

We have constructed the circuit in three op-amp stages using the schematic from the article by Engle & Wyttenbach. The first stage was basically the amplifying stage. As we can see from the graph, after the first stage, we have amplified the signal to a gain level that we can distinguish signal from noise. And we can see that the original signal and the amplified signal were 180 degrees out of phase in the

PSpice simulation. This can be explained since we have it in the inverting configuration. The second stage was there to adjust the DC offset of the optical sensor and the output of first stage. Also it served the purpose of inverting the output of the first stage as well. Clearly, we see the output signal now is in phase with the signal detected from the optical sensors. Since we use three photodiodes to pick up signals from the six strings, we have tried to simulate the circuit at three different frequencies as 100Hz, 500Hz, and 1kHz. After getting the signal from three photodiodes, we have the third stage which summing all of the three signals to output one signal so that we can feed into the audio amplifier. As we see from the graph, it really summed all the signals at different frequencies together and filtered using low-pass filter.

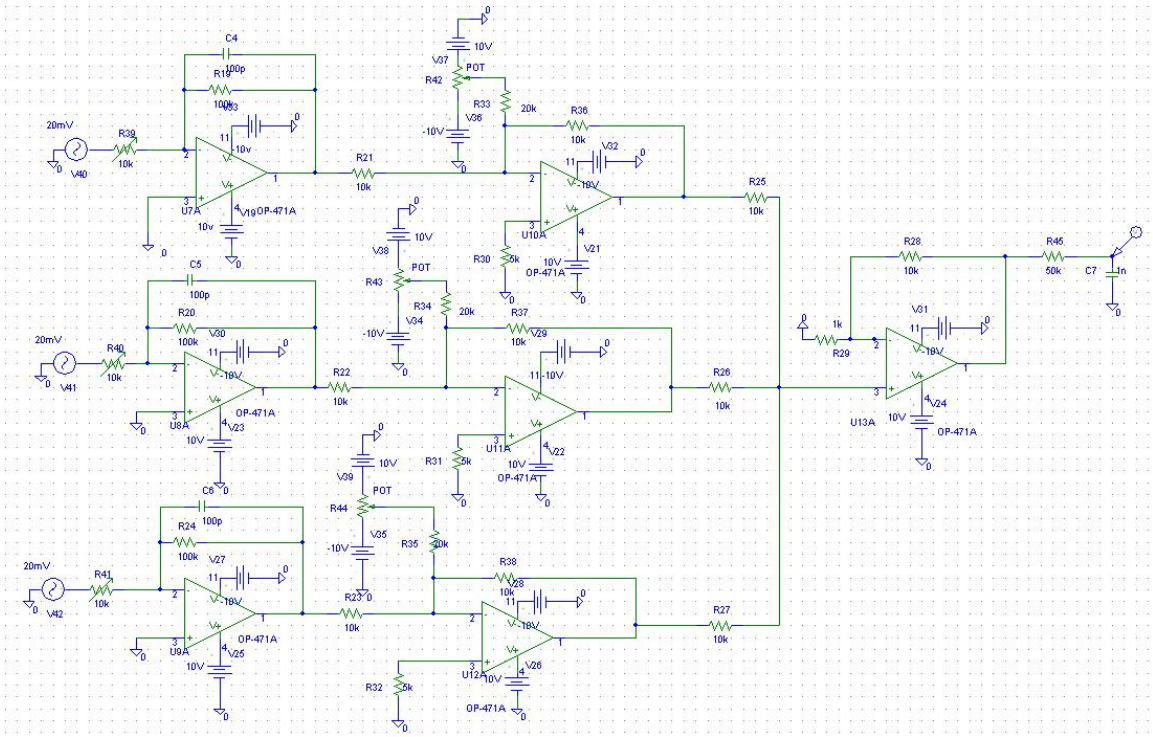

Figure 1: PSpice Schematic

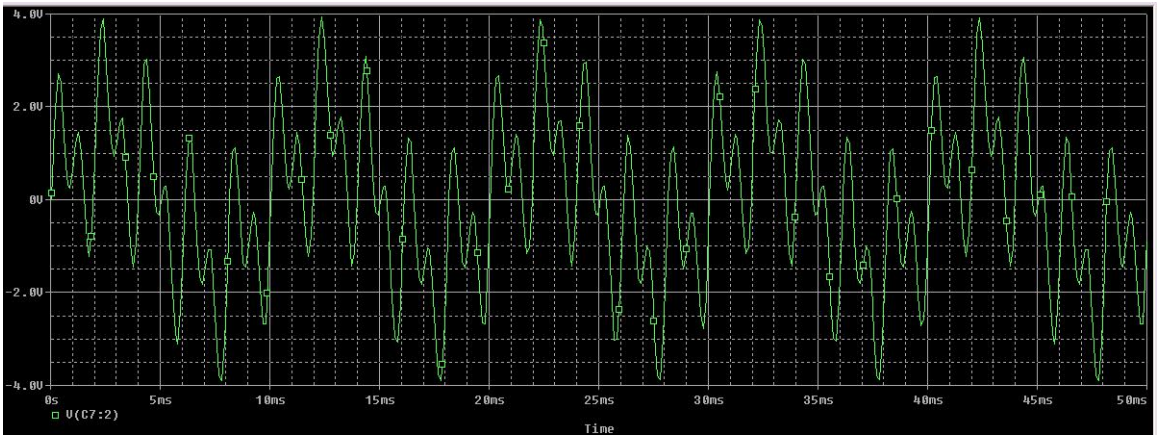

Figure 2: PSpice Simulation Final Output in Time Domain

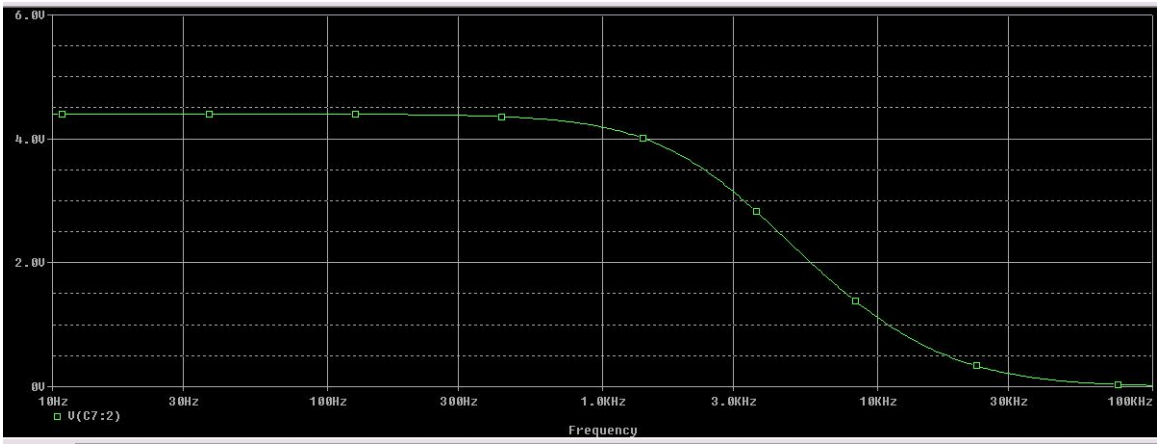

Figure 3: PSpice Simulation of Final Output in Frequency Domain

Final Circuit Construction on Breadboard:

After constructing our circuit according to the schematic from the article by Engle & Wyttenbach on breadboard, the final output signal was distorted with 1MHz noise from the power supply of the op-amps. Therefore, the circuit was further improved to reduce the high frequency noise and power supply noise by installing 0.01µF capacitors between the power supply pins of the op-amp to the ground. At the inverting inputs of the first stage, potentiometers are placed to adjust the gain from 150-500mV peak to peak for each optical sensor. They are also placed at the second stage to adjust the high DC offset resulting from the photodiodes to prevent saturation of the op-amp. Then, the combined signal is amplified again at the summing stage. In order to filter the unwanted high frequencies, we use 50KΩ resistor and 1nF capacitor to construct the passive filter.

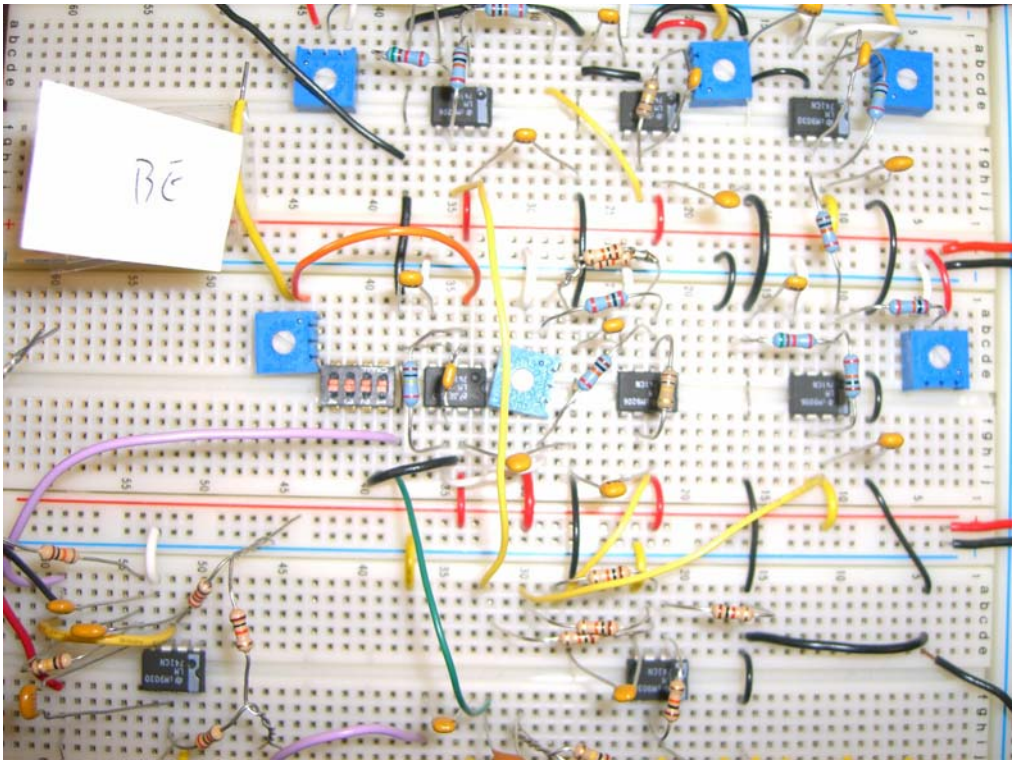

Figure 4. Actual layout of circuit on breadboard

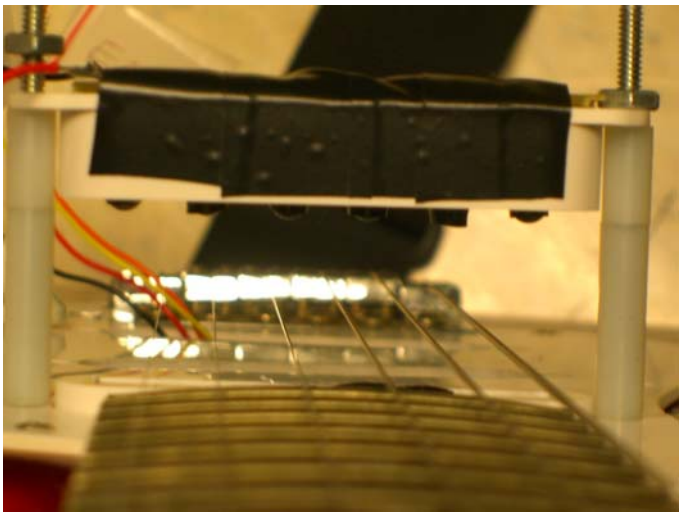

Figure 5. Construction of our transmission method prototype pickup.

Output Waveforms

The following waveforms are experimental results using our optical pickup with the transmission method.

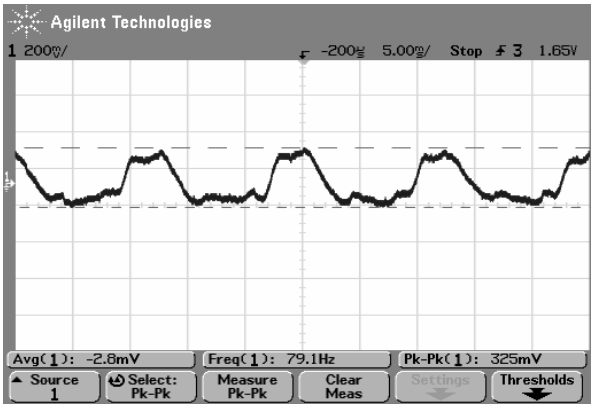

String-E (Low E)

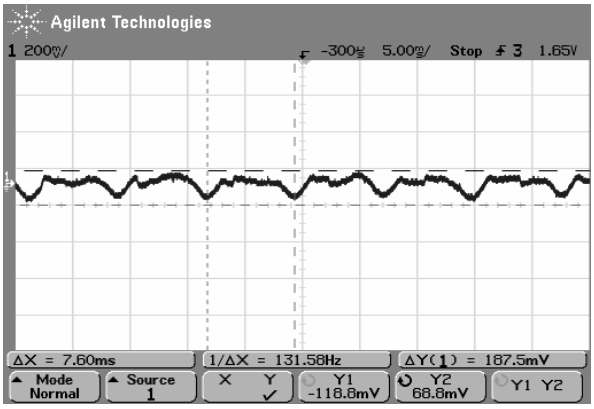

String-D

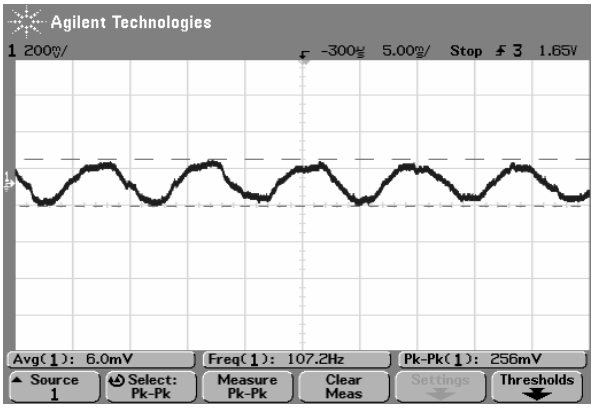

String-A

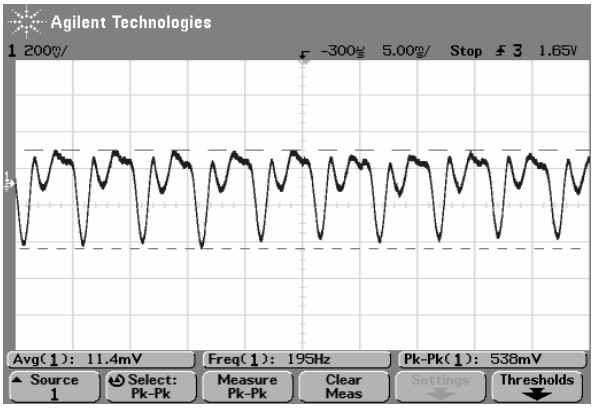

String-G

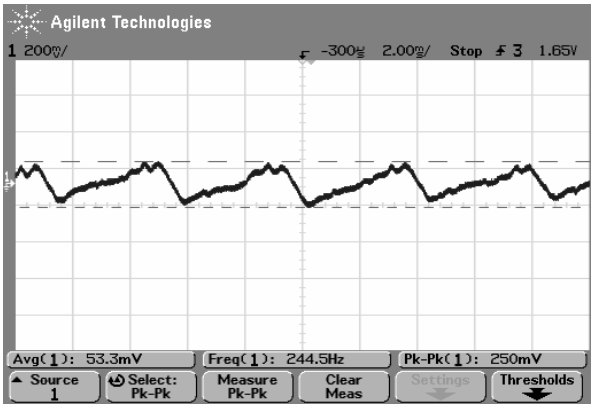

String-B

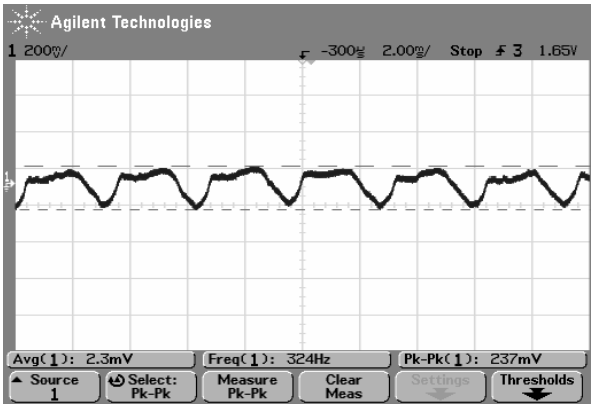

String-E (High E)

The following waveforms are experimental results obtained using a double humbucker magnetic pickup.

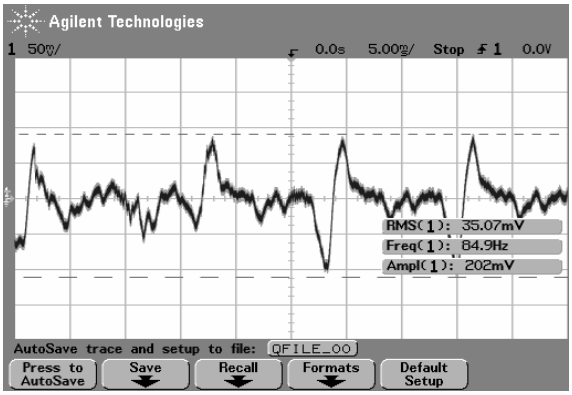

String-E (Low E)

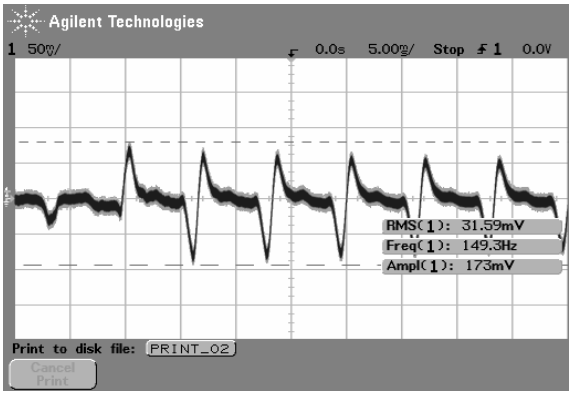

String-D

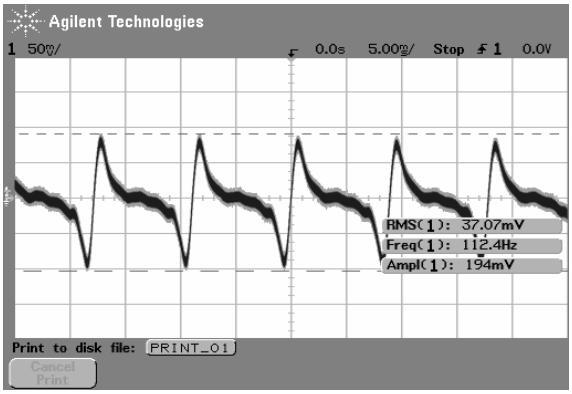

String-A

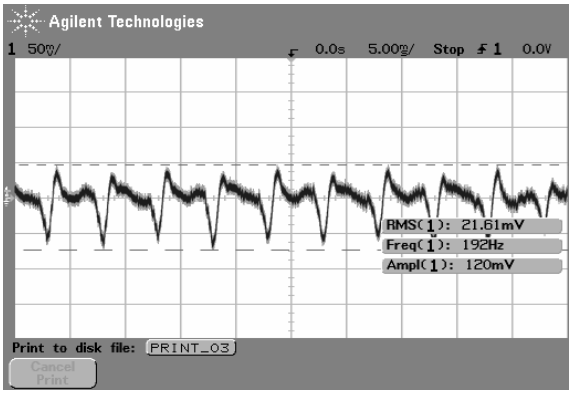

String-G

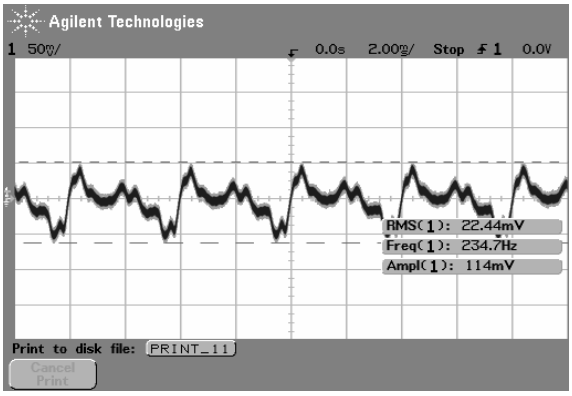

String-B

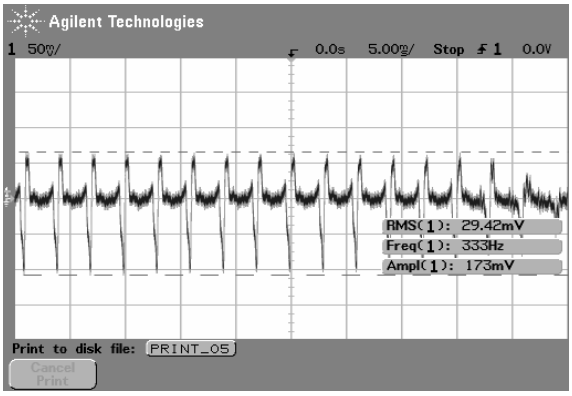

String-E (High)

Results

Results						
Experimental			Reference			
Optical pickup			Double Humbucker			
String	Magnitude	Frequency	Magnitude	Frequency	Error compared	to Reference (%)
(Open String)	(mV peak to peak)	(Hertz)	(mV peak to peak)	(Hertz)	Magnitude	Frequency
E	325	79.1	202	84.9	-60.89108911	6.831566549
A	256	107.2	194	112.4	-31.95876289	4.62633452
D	187.5	131.58	173	149.3	-8.38150289	11.8687207
G	538	195	120	192	-348.3333333	-1.5625
B	250	244.5	114	234.7	-119.2982456	-4.175543247
E	237	324	173	333	-36.99421965	2.702702703

The large percentage error in the resulting magnitude was largely due to the fact that we could not strike the strings consistently enough to produce the same level of vibration, therefore resulting in the large variation in the peak-to-peak magnitude from the output of the pickup. There are two major contributing factors for the large percentage error in the frequency measurements. First, in order for us to implement the prototype optical pickup, we had to constantly take off and restring the strings. Therefore, resulting in the strings being out of tune. The second factor being that it was very difficult to measure the frequencies of the vibrations using the oscilloscope, as the output amplitude reduced rather quickly and the oscilloscope required the output to be maintained at a certain level in order to measure the frequencies.

Analysis

We deviated from our initial design of reflection method to the transmission method. The reasons for the change was that there was too much ambient noise due to the surrounding lighting, especially with the fluorescent lighting, which added white noise with the frequency of 120 Hz and 50 mVpp. Additionally, the pickup also detected noise arising from the AC outlet, which provided additional noise with frequency of 60Hz. We were able to reduce the fluorescent noise by turning off all surrounding lights, but that does not provide us with a practical solution. Due to the broad spectrum of the fluorescent noise, one potential solution is to use higher power light sources. With the higher intensity output, we will be able

to create reflections with higher intensity, therefore allowing us to distinguish the large spikes in intensity as our usable signal.

In order to minimize the circuit power consumption and avoid clipping at different stages of the circuit, we added the potentiometers to adjust the gain of the amplification stage and also the DC offset of each stage. Infrared LEDs are not good choices for the reflection method because the output spectrum is not focus enough to generate usable reflection. Additionally, the wide numeric aperture of the LED output leads to destructive interference between each string. Another contributing factor to the failure of the reflection method is that in order for the sensor to detect the vibrations of the strings, we need to keep the exposed areas on the sensors relatively small. Small sensing areas not only help us detect the vibrations better, but also improve our circuit efficiency by lower the DC offset of the signals.

Potential improvements for the design could include using either a lens that will focus the light source more precisely on each string, hence leading to maximum reflection from the strings. The potential drawback of focusing the light to a very small area is that the strings do not always vibrate at the same place. That is to say, sometimes the player will needs to move the string in order to create a different sound. The design could also employ a noise cancellation circuit so that we can eliminate the ambient noise. The noise cancellation circuit would include a separate set of LED and sensor to detect the background noise without detecting any vibrations of the strings. We can then invert the output of the noise reference circuit and feed the output into the summing amplifier. We could also place different polarized lenses as an optical filter for the detected signal. By using polarized light to detect the vibration, we can eliminate the average power of the noise signal. We can also enclose the pickup in order to eliminate background noise from the lights around the guitar, but this would impede the way the player would play the guitar. Finally, we can also coat the strings using more highly reflective materials, i.e. silver or aluminum, in order to improve the overall reflection from the strings.

Summary

Quality sounds are difficult to produce, especially for an electric guitar. The typical magnetic pickup is easily interfered by the surrounding magnetic sources. To minimize this phenomenon, we came up with the design for an optical pickup system. The important specification of the optical pickup is that it will not interfere with the way a musician plays a guitar. The optical pickup will need to filter out the undesirable light from other light sources from the stage. The main goal of this project is to minimize the noise that is generated from the magnetic pickup. The pickup will detect signals from the strings and output the signals as audio signals. The main goals of this project includes picking up signals from the strings using light source and photodiodes, outputting a range of audible frequency of 20Hz to 20kHz, and not to modify the traditional way of playing an electric guitar. However, we were not able to meet the last specification as we changed our detection method from reflection to transmission. Our system is broken up into three subsystems, which included the detection stage, the amplification stage, and the summing stage. We were able to create a usable output that can be connected to an audio amplifier and produce sound. However, we were unable to detect the higher harmonics of the strings due to our filter that we used to

lower the humming noise from the pickup. Another drawback of our design was that our pickup would also interfere with the player's fingers due to the placement of the LEDs.

Bibliography

Engel, J. E. and Wyttenbach, R. A. (2001).
An optoelectronic sensor for monitoring small movements in insects. *Florida Entomologist*. 84, vol. 3, 336-343.

AN OPTOELECTRONIC SENSOR FOR MONITORING SMALL MOVEMENTS IN INSECTS

JEFF E. ENGEL[1] AND ROBERT A. WYTTENBACH
Department of Neurobiology and Behavior, Cornell University, Seeley G. Mudd Hall
Ithaca NY 14853-2702, USA

[1]Present address: Department of Biological Sciences, Western Illinois University
1 University Circle, Macomb IL 61455, USA

ABSTRACT

Optical movement detectors are often used in laboratory studies of insect behavior. They offer advantages of time resolution and ease of analysis compared with video. However, design and construction have rarely been described in enough detail to allow the devices to be built easily by others. We describe a simple optoelectronic system for measuring rapid movements in one dimension, such as the protraction of an insect leg. The leg casts a bar-shaped shadow onto a photodiode chip that is masked to expose a triangular area. Movement of the leg changes the total area of the triangle that is shaded. A preamplifier converts the change in photoelectric current to a voltage signal. The preamplifier includes an optional circuit for removing 120 Hz ripple resulting from AC-powered light sources by subtracting the output of a second, reference photodiode. We have used the system to quantify leg movements in an acoustic startle response of a field cricket (*Teleogryllus oceanicus* LeGuillou). This system could be adapted for a wide range of other applications in laboratory and field research.

Key Words: leg motion, position detector, photodiode, optoelectronic photodetector, cricket acoustic startle response

RESUMEN

Detectores ópticos de movimiento han sido usados frecuentemente en estudios de comportamiento de insectos en el laboratorio, donde ofrecen ventajas de resolución de tiempo y facilidad de análisis comparado con video. Sin embargo, su diseño y construcción han sido raramente descritos en suficiente detalle para permitir que otros puedan construir estos aparatos fácilmente. Describimos un sistema optoelectrónico para medir movimientos rápidos en una dimensión como la protracción de una pata de insecto. La pata forma una sombra en forma de barra a un chip fotodiodo que esta cubierto para exponer una área triangular. El movimiento de la pata cambia el área total del triangulo que esta sombreado. Un preamplificador convierte el cambio en corriente fotoeléctrica a una señal de voltaje. El preamplificador incluye un circuito para nulificar ondulación de 120 Hz de fuentes de luz con electricidad AC al restar la producción de fotodiodo de referencia. Hemos usado el sistema para cuantificar movimientos de pata en una respuesta de susto acústica del saltamontes *Telegryllus oceanicu* (LeGuilou). Elementos de este sistema pueden también ser adaptados para otras aplicaciones en estudios de laboratorio y de campo.

Optoelectronic position detectors may be used to quantify behavior in a wide variety of settings. Optoelectronic methods have two advantages over video: (1) Temporal resolution is not limited by video frame rate, and (2) The detector can measure a single parameter of movement or position that would require extensive labor or computer processing to extract from video records. Descriptions of optoelectronic devices in the biological literature generally emphasize the unique features of a particular detector without providing details of design and construction. Potential users may be discouraged from applying these methods if they lack the practical electronics background to adapt the circuits found in electronics cookbooks or technical literature from chip manufacturers. We describe a photodetector and amplifier designed for monitoring leg protraction in a tethered flying Polynesian field cricket (*Teleogryllus oceanicus* LeGuillou), and readily adaptable to other uses as described in Results and Discussion.

We are studying an ultrasound-induced escape response in crickets, a flight turn that is a defense against echolocating bats (Moiseff et al. 1978). A cricket is flown on a tether and given pulses of ultrasound from a loudspeaker mounted to its left or right. We monitor one component of the startle response, a lateral outward swing of the metathoracic leg contralateral to the source of ultrasound (May & Hoy 1990). This movement has ~30 ms latency and 45 to 65 ms time-to-peak, too rapid to quantify with conventional video. We designed an

optoelectronic detector to convert leg position to a continuous voltage signal that indicates position without the need of further processing. The design uses a triangular detection surface in such a way that movement of the leg's shadow produces a change in illumination, and incorporates a method for canceling the light ripple that is found in AC powered light sources. These features are demonstrated below (Results and Discussion).

This device has performed well in measurements of the cricket acoustic startle response (e.g., Engel & Hoy 1999). Movement of the metathoracic femur is faithfully represented as a voltage signal, and ripple due to AC line power is eliminated. The circuit is conservatively designed using parts that are readily available in electronics stockrooms or outlets such as Radio Shack (electronics vendors and photodiode suppliers are listed in Appendix A). The circuit and photodetector are described in sufficient detail to be built as they are, and they could also be adapted to a variety of other purposes. It is our hope that descriptions such as this will enable more widespread use of optoelectronic methods in entomology and in biological research in general.

Materials and Methods

This section describes the essential features of design and construction. Additional notes are provided in Appendix A, along with a list of parts and suppliers. For an introduction to electronic components, schematic diagrams, and assembly techniques see Mims (2000) or other basic texts.

Movement Detector

There are several approaches to optoelectronic movement detection. (1) Use of small arrays of discrete photodectors to determine the position of a light or shadow (e.g., Kittmann 1991; Erber & Kloppenburg 1995; Roberts 1995). (2) Use of a linear position-detector photodiode chip (e.g., Helversen & Elsner 1977; Hedwig 1988; Kelly & Chapple 1988; Mayer et al. 1988; Hedwig & Becher 1998). (3) Use of a simple photodetector chip to measure a moving shadow (e.g., Meyer et al. 1987; Rüsch & Thurm 1989; Clark et al. 1990; Götz 1987; May 1990). The first two approaches are relatively complicated, and reports have not given sufficient details for circuits to be constructed readily. Our device is a refinement of the third approach.

If a shadow has a single moving edge, then a simple rectangular photodiode can act as a position sensor because the shaded area varies linearly with position, resulting in a linear change in the output of the photodiode (Meyer et al. 1987; Rüsch & Thurm 1989; Clark et al. 1990). However, when the shadowing object has both leading and trailing edges, as an insect appendage does, the shadow's area does not change with position. In this case, a mask with a triangular or crescent-shaped opening can be interposed into the light path between the appendage and the photodetector (Götz 1987; May 1990; May & Hoy 1991). As the appendage's shadow moves to a wider part of the triangular opening, the shaded area of the photodetector increases. This makes a simple and effective position indicator, as we show below (Results and Discussion). In the cricket leg position detector described here, a triangular mask is affixed directly to the photodetector surface, as in May (1990), eliminating the need for optics between the mask and the photodetector, as in Götz (1987).

Our photodetector uses a 10×20 mm unpackaged silicon photodiode chip (EG&G Vactec, St. Louis, MO, VTS 3081). A predecessor of our design used a CdS photoconductor chip in a voltage-divider circuit (May 1990). We chose a silicon photodiode because of its superior frequency response and uniform surface geometry compared with CdS photoconductors (*Photodiodes*, Hamamatsu, Bridgewater, NJ, 1997). For structural support, the chip is fastened with double-sided foam tape to an IC (integrated circuit) mount (Fig. 1C) with the chip lead wires soldered to the pins. A second IC mount serves as a socket, with wires leading to the amplifier. In our setup this socket is attached to a swivel ball joint mounted on a rod. The small size of the detector assembly allows it to be placed around electrodes for simultaneous neural and behavioral recording from a flying cricket (J.E.E., unpublished data) and minimizes disturbance of the acoustic field.

The photodiode chip is masked with black graphics tape (Chartpak, Leeds MA) to leave a triangular area exposed (Fig. 1C). The tethered cricket is illuminated from above with a fiber-optic light guide, so that the metathoracic femur casts a bar-shaped shadow onto the photodetector, which is 1 to 2 cm below the leg. As the leg pivots laterally, its shadow moves to a wider part of the triangle. The area of the shadow on the triangle, and the resulting change in photocurrent from the photodetector, are proportional to the magnitude of lateral movement (see Results and Discussion).

Position Amplifier

A photodiode produces a current directly proportional to the amount of illumination (*Photodiodes*, Hamamatsu, Bridgewater NJ, 1997, p. 5). The amplifier (Fig. 1A) converts this current signal to a more conveniently analyzed voltage signal with the desired level of gain. The first operational amplifier (op amp), IC1, of the position amplifier converts current (i) to voltage (v). The current-to-voltage gain is determined by feedback resistance R, with the relationship $v = i\mathrm{R}$. The value of R is best chosen by trial and error

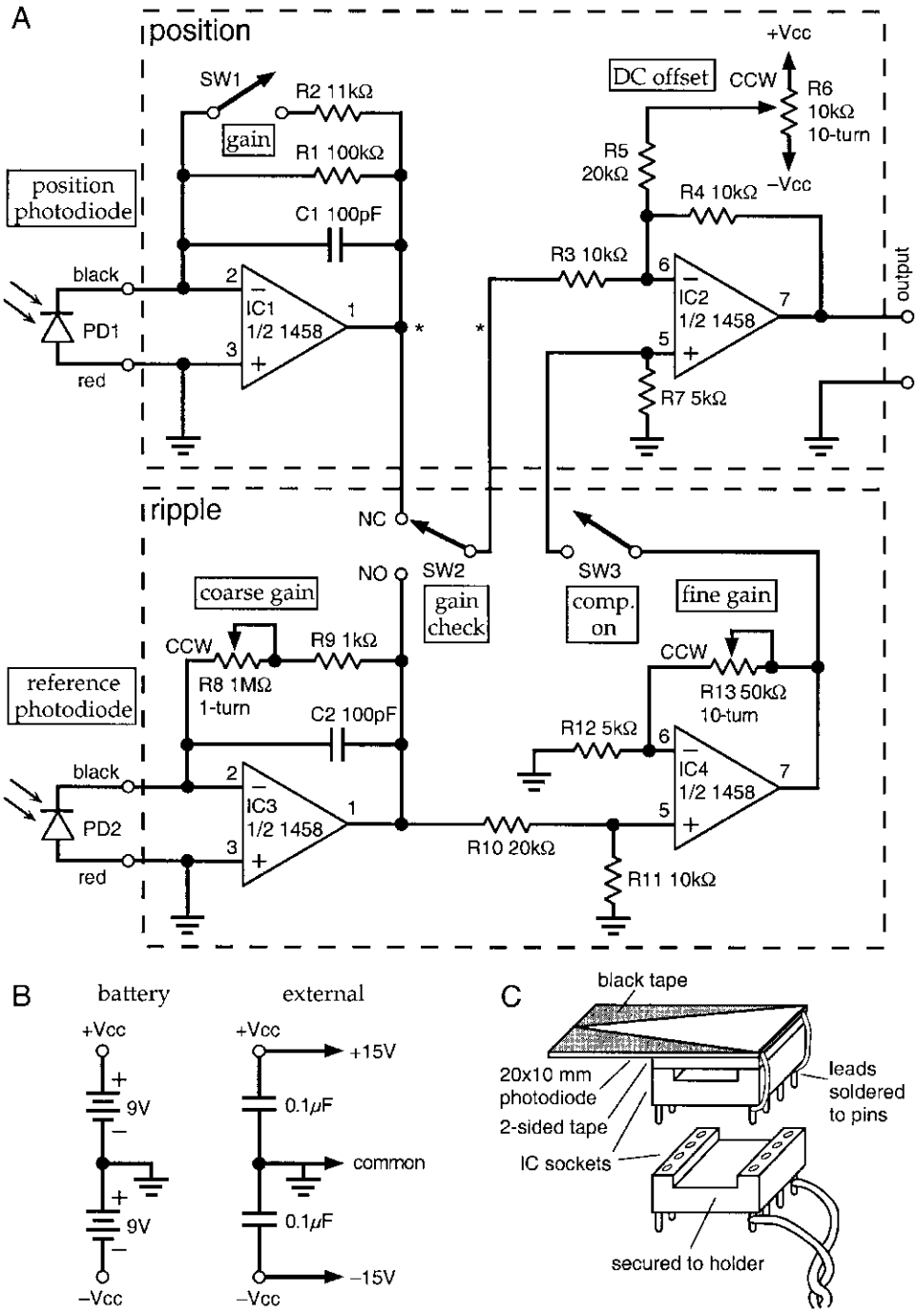

Fig. 1. Position detector design. A. Amplifier circuitry. The two components, the position amplifier and the ripple-compensation amplifier, are outlined in dashed boxes. If the position amplifier is built alone, the points indicated by asterisks are connected. Each IC is half of a 1458 dual op-amp package, with numbers indicating pin assignments. In R6, R8, and R13, CCW indicates the lead that has zero resistance when the potentiometer is turned fully counterclockwise. Abbreviations: C, capacitor; CCW, counterclockwise; IC, integrated circuit; NC, normally closed; NO, normally open; PD, photodiode; R, resistor; SW, switch; Vcc, power supply voltage. See Appendix A for a list of parts. B. Power can be provided by two 9 V batteries (left) or an external DC power supply not exceeding ±18 V (right). Open circles labeled +Vcc and –Vcc are nodes to be connected to the op-amp packages (pins 8 and 4, respectively) and to the terminals of R6. C. Photodetector. A photodiode is masked to expose a triangular area and mounted to an 8-pin integrated circuit (IC) socket for physical support. A second IC socket serves as a connector to the amplifier.

because the appropriate gain depends upon the strength of the light and the size and sensitivity of the photodiode. In our setup, R is 10 or 100 kΩ, set by R1 or by R1 and R2 in parallel ($R = R1 \times R2/(R1 + R2)$). If lower light levels or a smaller photodiode are used, an R of several megaohms might be required. Switch SW1 allows switching between two gain settings during operation.

The second op amp (IC2) adds a DC offset to the signal, allowing the baseline of the output voltage to be adjusted to the middle of the input range of a recording device or oscilloscope. Potentiometer R6 controls the amount of DC offset, functioning as a voltage divider together with resistor R5. IC2 also inverts the voltage signal. In our setup the anode of the photodiode (red lead) is connected to the positive input of IC1 so that a leg swing away from the body (which increases shadow area) causes a negative photocurrent fluctuation leading to a negative voltage signal. IC2 inverts this so that the lateral leg swing of an escape response produces a positive output signal. If a negative-going signal were desired, the photodiode leads would be connected in the reverse orientation. Either orientation is permissible because the photodiode is not voltage-biased in this circuit.

Ripple Compensation

Light from AC-powered lamps can have a pronounced ripple at twice the line frequency (120 Hz in North America). In our setup a standard fiber optic light source (Dolan-Jenner, Woburn MA, Series 180) provides strong illumination with low heat and allows the lamp housing to be kept outside of the Faraday cage. However, the optic ripple is considerable (Fig. 2B).

This ripple can be cancelled electronically (Fig. 2B). A reference photodiode is placed near the movement detector but out of the path of the cricket's shadow. Both photodiodes pick up the light ripple, and the movement detector also senses a change in illumination as the leg moves. Ripple is eliminated by subtracting the reference signal from the movement signal. The reference photodiode need not be identical to the movement detector photodiode, nor need their levels of illumination be matched, because the gain of the reference signal can be adjusted over a large range. Appendix B shows a straightforward method for adjusting the gain so that the reference signal exactly cancels the ripple in the movement signal.

The first op amp (IC3) of the ripple compensation amplifier converts the reference photocurrent to a voltage signal (Fig. 1A). Coarse gain control is adjusted at this stage by potentiometer R8, and fine gain control is adjusted at the second op amp (IC4) by potentiometer R13. The reference signal is subtracted from the movement signal by feeding it into the positive input of the position amplifier's second op amp (IC2). To build the position amplifier only, without ripple compensation, connect the points marked with asterisks in Fig. 1A and omit all components in the ripple section.

An alternative to electronic subtraction of light ripple is use of a DC-powered light source (Fig. 2B). We converted our Dolan-Jenner fiber optic light source to DC power by cutting the wires that connect the variable transformer to the lamp, diverting the transformer output to a DC converter in a separate housing, and feeding the DC power back to the lamp. The DC converter consists of a full-wave rectifier protected with a heat sink, with the output leads connected across 93,000 μF of capacitance in parallel to the lamp. Because the cost of capacitors increases with voltage rating, 15 V capacitors were used and the power supply transformer is kept in the lower end of its range. This provides ample light for our purposes.

Testing Linearity and Ripple Compensation

To show that the voltage signal is a linear function of shadow area, a metal rod (2 mm diameter) was mounted on a motor so that it swung across the photodetector 1.5 times per second (Fig. 2A). The far edge of the photodiode was 108 mm from the axle, giving the rod a speed of 1 m/s as it passed over the photodiode. The output of the amplifier was recorded without ripple compensation and with electronic compensation (Fig. 2B, left and center traces). Then, with electronic compensation inactivated, the DC converter was switched into the lamp power supply without otherwise altering the setup (Fig. 2B, right trace).

To demonstrate adjustment of ripple compensation (Fig. 3), the position photodetector was set up to monitor the left metathoracic femur of a tethered flying cricket. The reference photodetector was a fragment of a broken solar cell (~0.15 cm^2 lit area). Voltage outputs were digitally sampled at 5 kHz and 0.3 mV resolution. To show escape responses in both directions (Fig. 3E), a second photodetector and amplifier (also with ripple compensation) monitored the right metathoracic femur. Both photodetectors were in place throughout the series of records in Figure 3. Ultrasound pulses were 20 kHz carrier frequency, 10 ms duration. The cricket preparation and acoustic setup have been described elsewhere (May & Hoy 1991; Wyttenbach & Hoy 1997); as previously, hind wings were cut short so they would not interrupt the light path.

Results and Discussion

Linearity of Movement Detection

Photodiode chips have a uniform photosensitive surface (in contrast to photoconductors, which have a zigzag ribbon of photosensitive material).

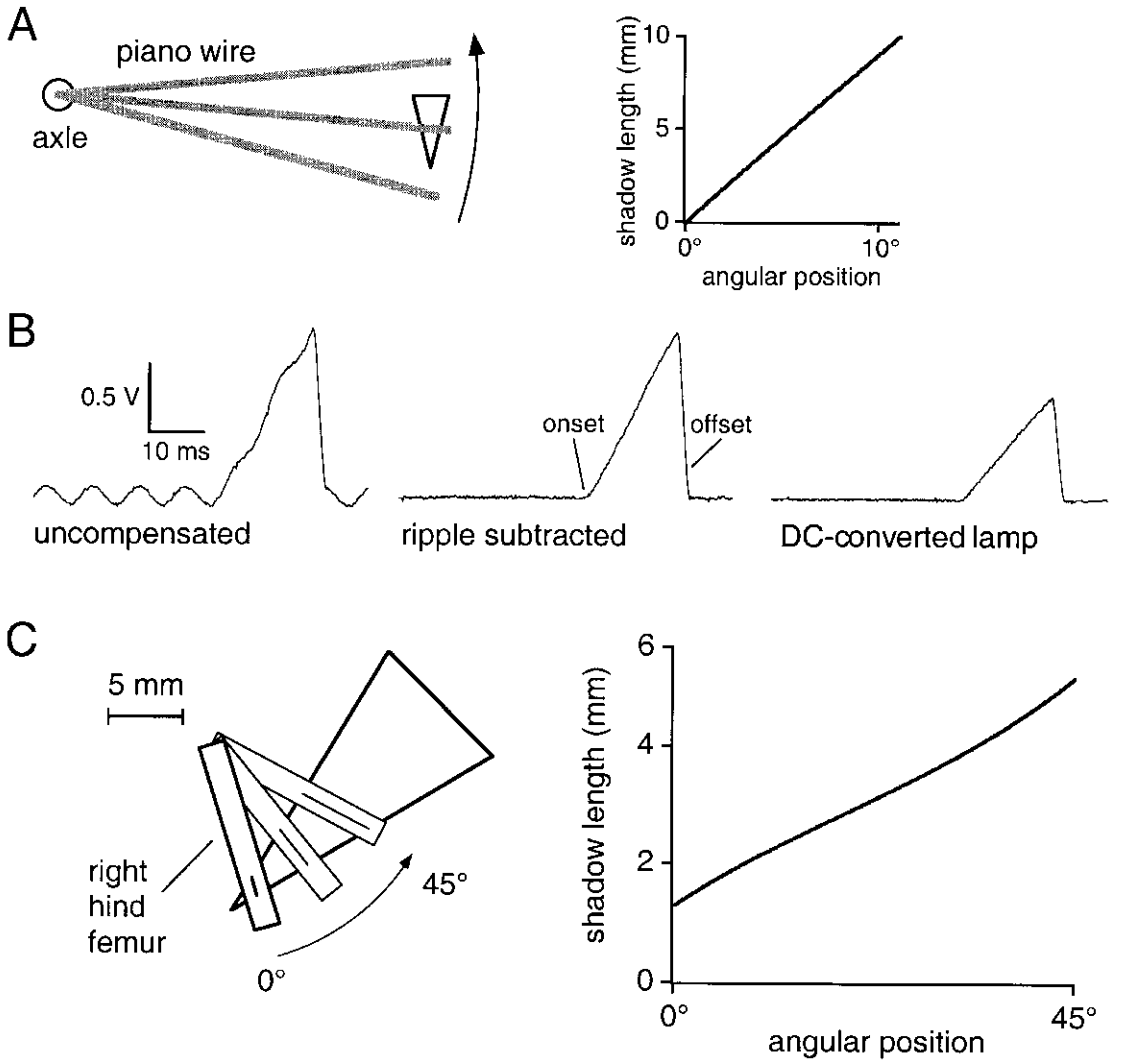

Fig. 2. System performance. A. Linearity testing. A 2mm thick rod passed across the photodiode at a speed of 1 m/s. The shadow's area is proportional to its length on the triangular photodetector. The graph shows the calculated length of the rod's shadow as a function of its angular position. B. Ripple compensation. Using the above setup, records were made without compensation for light ripple (left), with electronic compensation (center), and with the light source converted to DC operation (right). The two compensated traces are linear, as predicted in part A. Onset and offset are not instantaneous because of the 2 ms time required for the full width of the shadow to enter or leave the triangle. C. Calculations for a cricket leg. The metathoracic femur is essentially rectangular when viewed from above. As long as its shadow crosses the entire triangle, the area of the shadow on the triangle is proportional to its midline length. The calculated midline length is an approximately linear function of angular position over a range of at least 45°.

The photocurrent output of a photodiode should be a linear function of the area that is illuminated (or the area that is shaded). To test this, a rod about as thick as a cricket hindleg femur was moved across the triangular detector such that the area of the rod's shadow on the photodetector increased uniformly with time (Fig. 2A). The output signal increased uniformly as well (Fig. 2B), indicating that the output signal is a linear function of shaded area.

For the output signal to faithfully indicate leg deflection, however, the shaded area itself must be a linear function of the angular movement of the femur. This assumption holds rather well, provided that the photodetector is positioned so that the femur is perpendicular to the axis of the triangle when the femur is in the middle of its range of motion (Fig. 2C). This was demonstrated with a trigonometric model. The shadow of the femur on the photodetector can be represented as a

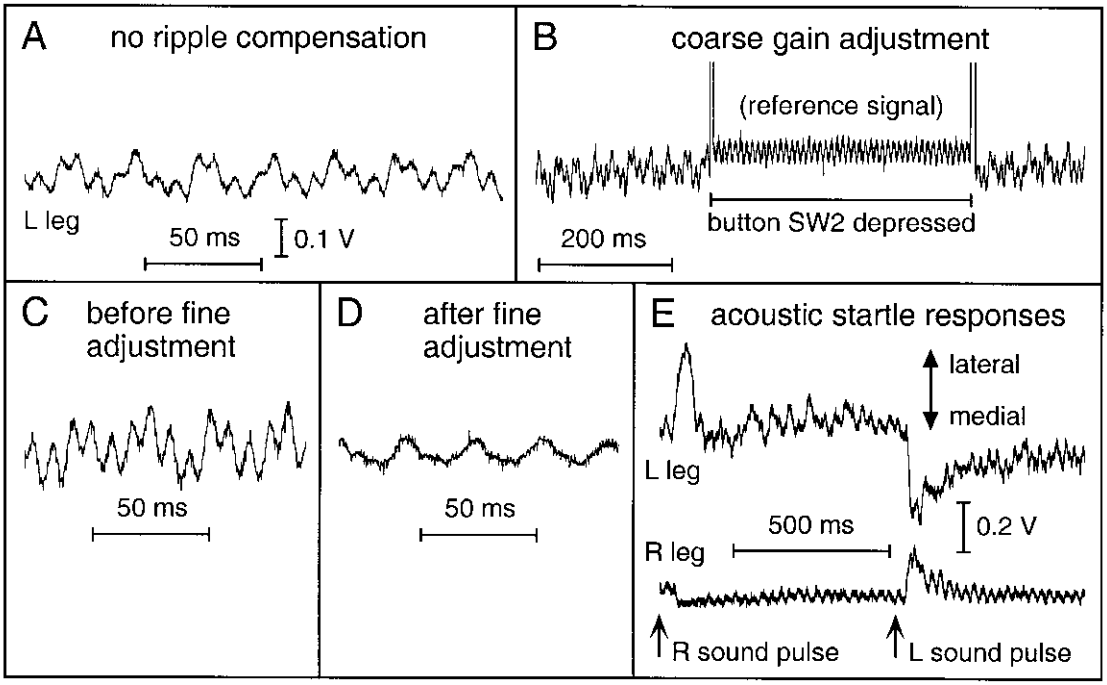

Fig. 3. Adjustment of ripple compensation. The position photodetector monitored the left metathoracic femur of a tethered flying cricket. Voltage scale of Panel A applies to all panels except E. A. Signal without ripple compensation (SW3 open). Fluctuations are a combination of light ripple (120 Hz) and leg vibration due to wing beats (~35 Hz). B. Coarse gain (R8) is adjusted to minimize the jump of the trace when the reference signal is switched into the movement amplifier path using pushbutton SW2. C. Ripple compensation is engaged (SW3 is closed) but fine gain has not been properly balanced to eliminate ripple. D. Fine gain (R13) has been adjusted to minimize ripple. Remaining fluctuations reflect real leg movements due to wing vibration. E. Escape responses in the same preparation. A second photodetector and amplifier monitored the right metathoracic femur. For both legs, a positive voltage signal indicates lateral deflection. Ultrasound pulses from the right and then the left side (arrows) evoked outward lateral movements of the contralateral hind legs. Differences in amplitudes of vibration and escape response between the two legs were real (not an artifact of using two different detectors and amplifiers).

bar of uniform thickness (Fig. 2C). As long as this bar crosses two sides of the triangle, the area of the shadow on the triangle will always be proportional to the length of the shadow at its midline. The trigonometric model shows that with optimal positioning of the photodetector, this midline length is an approximately linear function of angular movement over a range of 45° (Fig. 2C) (leg movement in the escape response rarely exceeds 20°, Miles et al. 1992).

In our experiments it is not necessary to determine the relationship between the degree of movement and the amplitude of the voltage signal. We are concerned with relative changes in the amplitude of the leg response in a habituation paradigm. The habituated responses are simply normalized to control responses within the same trial. However, the position-to-voltage scale for a trial could be determined by moving the cricket's femur to different angles using forceps, recording the resulting voltage output levels, and measuring the leg angles from videotape recordings made during the same manipulations.

Compensation for Light Ripple

When illumination is provided by an AC light source, the optic ripple adds substantial "noise" to the movement signal (Fig. 2B; Fig. 3A). We compared two methods for eliminating this ripple, subtracting it electronically or adding a DC converter to the light source. Both approaches worked well (Fig. 2B). Electronic subtraction is the most flexible method because any source of light can be used. The gain of the reference signal must be calibrated with each use, but this can be done by a simple procedure (Appendix B, Fig. 3). DC illumination is the more direct method. DC illuminators may not be commonly found in many laboratories, but an AC unit can be converted to DC operation as described above.

Other Applications

This design includes a photodetector that converts angular position to a photoelectric signal, a photodiode amplifier with DC offset compensa-

tion, and a second amplifier incorporating continuous gain adjustment and subtraction of its output from the first amplifier. These three components could be adapted to a variety of uses. (1) The photodetector could monitor other appendages such as wings or antennae, and the shape of the mask could be altered as needed to track the movement of a particular appendage (Götz 1987). Photodiodes come in several sizes, from 1×3 to 20×20 mm, and can be connected in parallel if larger areas are needed (larger solar cells may also be used). (2) The position amplifier could be used with an unmasked photodiode in applications where the timing of movement is of more interest than its spatial characteristics. For example, in the laboratory an unmasked detector could indicate the wing beat frequency of a tethered insect or detect an animal's transit past a point in a cage. The latter application could be adapted in the field for counting visits to a colony or lure. (3) The ripple compensation amplifier could serve as the basis for other applications requiring differential processing, such as automatic compensation for variation in ambient light levels. Another potential application is dual-photodiode movement detection (Crawford & Fettiplace 1985; Iwazumi 1987), in which a shadow overlaps two adjacent photodiodes and moves onto one as it moves off of the other.

The advantages of fine temporal resolution and simplicity of analysis mentioned in the Introduction make optoelectronic movement detection attractive for a variety of applications. We hope that this description will provide a point of entry for workers without much electronics background, and a starting point for those with more experience who can modify the design to suit their particular applications.

ACKNOWLEDGMENTS

We thank Bruce Land for comments on circuit design, and Ronald R. Hoy, in whose laboratory we carried out this project (both are of Cornell University).

REFERENCES CITED

CLARK, B. A., R. HALLWORTH, AND B. N. EVANS. 1990. Calibration of photodiode measurements of cell motion by a transmission optical lever method. Pflügers Arch. 415: 490-493.

CRAWFORD, A. C., AND R. FETTIPLACE. 1985. The mechanical properties of ciliary bundles of turtle cochlear hair cells. J. Physiol. (London) 364: 359-379.

ENGEL, J. E., AND R. R. HOY. 1999. Experience-dependent modification of ultrasound auditory processing in a cricket escape response. J. Exp. Biol. 202: 2797-2806.

ERBER, J., AND P. KLOPPENBURG. 1995. The modulatory effects of serotonin and octopamine in the visual system of the honey bee (*Apis mellifera* L.): I. Behavioral analysis of the motion-sensitive antennal reflex. J. Comp. Physiol. A 176: 111-118.

GÖTZ, K. G. 1987. Course-control, metabolism and wing interference during ultralong tethered flight in *Drosophila melanogaster*. J. Exp. Biol. 128: 35-46.

HEDWIG, B. 1988. Activation and modulation of auditory receptors in *Locusta migratoria* by respiratory movements. J. Comp. Physiol. A 162: 237-246.

HEDWIG, B., AND G. BECHER. 1998. Forewing movements and intracellular motoneurone stimulation in tethered flying locusts. J. Exp. Biol. 201: 731-744.

IWAZUMI, T. 1987. High-speed ultrasensitive instrumentation for myofibril mechanics measurements. Am. J. Physiol. 257: C253-C262.

KELLY, T. M., AND W. D. CHAPPLE. 1988. An inexpensive, microcomputer-based system for recording movements in real time. J. Neurosci. Methods. 23: 35-42.

KITTMANN, R. 1991. Gain control in the femur-tibia feedback system of the stick insect. J. Exp. Biol. 157: 503-522.

MAY, M. L. 1990. Biomechanics of Ultrasound-Induced Steering in Tethered, Flying Crickets. Doctoral Thesis, Cornell University.

MAY, M. L., AND R. R. HOY. 1990. Leg-induced steering in flying crickets. J. Exp. Biol. 151: 485-488.

MAY, M. L., AND R. R. HOY. 1991. Habituation of the ultrasound-induced acoustic startle response in flying crickets. J. Exp. Biol. 159: 489-499.

MAYER, M., K. Vogtmann, B. Bausenwein, R. Wolf, and M. Heisenberg. 1988. Drosophila flight control during "free yaw turns". J. Comp. Physiol. A 163: 389-399.

MEYER, R., J. WIEMER, J. DEMBSKI, AND H. G. HAAS. 1987. Photoelectric recording of mechanical responses of cardiac myocytes. Pflügers Arch. 408: 390-394.

MILES, C.I., M. L. MAY, E. H. HOLBROOK, AND R. R. HOY. 1992. Multisegmental analyses of acoustic startle in the flying cricket (*Teleogryllus oceanicus*): Kinematics and electromyography. J. Exp. Biol. 169: 19-36.

MIMS, F. M. 2000. Getting Started in Electronics (3rd ed.). Radio Shack U. S. A. 128 pp. (Radio Shack item 62-5004).

MOISEFF, A., G. S. POLLACK, AND R. R. HOY. 1978. Steering responses of flying crickets to sound and ultrasound: Mate attraction and predator avoidance. Proc. Natl. Acad. Sci. USA 75: 4052-4056.

ROBERTS, W. M. 1995. Hummingbird licking behavior and the energetics of nectar feeding. Auk 112: 456-463.

RÜSCH, A., AND U. THURM. 1989. Cupula displacement, hair bundle deflection and physiological responses in the transparent semicircular canal of young eel. Pflügers Arch. 413: 533-545.

VON HELVERSEN, O., AND N. ELSNER. 1977. The stridulatory movements of acridid grasshoppers recorded with an opto-electronic device. J. Comp. Physiol. A 122: 53-64.

WYTTENBACH, R. A., AND R. R. HOY. 1997. Spatial acuity of ultrasound hearing in flying crickets. J. Exp. Biol. 200: 1999-2006.

Appendix A: Construction and Design Notes

Photodiode chips in sizes from 1 × 3 mm to 20 × 20 mm are available from Advanced Photonix (Camarillo, CA, 805-987-0146, www.advancedphotonix.com), Perkin Elmer (formerly EG&G Vactec; St. Louis, MO, 314-423-4900, www.perkinelmer.com) and Hamamatsu (Bridgewater, NJ, 908-231-0960, usa.hamamatsu.com). Solar cells of 20 × 40 mm are available from Edmund Scientific (Barrington, NJ, 800-728-6999, www.edsci.com) and Radio Shack (Fort Worth, TX, 800-843-7425, www.radioshack.com). Allied Electronics (Fort Worth, TX, 800-433-5700, www.alliedelec.com), Newark Electronics (Chicago, IL, 800-463-9275, www.newark.com), and Radio Shack are comprehensive vendors that carry all the remaining parts.

In addition to the two photodiodes, the circuit shown in Fig. 1 A requires the following parts: fixed 1/4 or 1/8 Watt resistors of 100 kΩ (R1), 11 kΩ (R2), 10 kΩ (R3, R4, R11), 20 kΩ (R5, R10), 5 kΩ (R7, R12), and 1 kΩ (R9); variable resistors of 10 kΩ (R6), 1 MΩ (R8), and 50 kΩ (R13); 100 pF capacitors (C1-2), type 1458 dual op-amp packages (IC1-4); SPST switches (SW1, SW3); SPDT momentary pushbutton switch (SW2); DPST switch (power on/off, not shown in Fig. 1). Note that R6 and R13 should be 10-turn potentiometers for greater precision in setting DC offset and ripple gain. Other parts needed to house the circuit include a case, circuit board, connection jacks (banana or BNC), and so on.

We used bipolar 1458 dual op amps (Radio Shack 276-038) because they are resilient and readily available. For biological applications requiring exceptional high-frequency or low-noise performance, this design could be refined by selecting high-performance op amps, by optimizing the feedback capacitance (C1), or by voltage-biasing the photodiode. Guidelines can be found in technical literature from photodiode manufacturers (e.g., *Photodiodes*, Hamamatsu, Bridgewater, NJ, 1997).

Resistors R1 and R2 should be at least 1 kΩ to prevent exceeding the op amp current rating, yet small enough to avoid saturating the op amp at high light intensities. The ideal values of R1 and R2 for a particular setup are best determined by trial and error. This process is made easier if R1 and R2 are plugged into an IC socket instead of being soldered directly to the circuit board. The range of gains available during normal use could be extended over several orders of magnitude by making SW1 a rotary switch and installing additional resistors. Capacitor C1 is included to prevent ringing. However, it should be noted that the feedback circuit is a low pass filter with a cutoff frequency of $f = [2\pi\ R1\ C1]^{-1}$; therefore C1 should be small enough to avoid filtering out biological signals of interest.

The maximum useful gain of the first op amp of the position amplifier is limited because the DC baseline resulting from overall illumination is amplified along with the signal due to movement. If movements of the leg shadow are small relative to the lighted area of the photodiode, the final output signal after DC compensation will also be small. This can be countered to some extent by reducing the unused lighted area of the photodetector as much as possible. At the second op amp, the baseline signal is subtracted using DC offset compensation. Therefore, an additional amplifier stage could be placed after the second op amp if more gain were needed. We have not found this to be necessary.

In the DC offset compensation circuit, R5 should not be much greater than R4 because the ratio R4/R5 is a gain factor that limits the available range of offset. At the same time, R5 must be greater than R6 to give R6 sufficient linearity as a variable voltage divider. A "voltage-follower" amplifier could be added as a buffer between R6 and R5 if desired. This would make the R6 voltage divider linear without regard to R5, and would also allow a larger R6 to be used (to reduce the current drain on batteries, for instance).

Appendix B: Adjusting Ripple Compensation

For electronic subtraction to be effective, ripple in the reference and position signals must have the same amplitude. This is achieved by adjusting the gain of the ripple compensation amplifier through the following simple procedure:

1. *Adjust position detector amplifier.* Set oscilloscope to DC mode and confirm that ripple compensation is not engaged (SW3 is open). Set the position amplifier gain (SW1) and adjust DC offset (R6) to center the signal (Fig. 3 A).

2. *Adjust coarse gain of reference signal.* Use the momentary pushbutton (SW2) to switch the reference signal into the movement amplifier path (Fig. 3 B). Adjust R8 to minimize the jump in the oscilloscope trace as SW2 is pressed and released.

3. *Adjust fine gain to minimize ripple.* Switch the oscilloscope to AC mode and engage ripple compensation by closing switch SW3 (Fig. 3 C). Adjust R13 to minimize the size of the ripple (Fig. 3 D). In this example (Fig. 3 D), light-source ripple has been effectively eliminated. The remaining "noise" is biological in origin (leg vibration due to wing beats).

4. *Readjust DC offset.* Return the oscilloscope to DC mode and adjust DC offset (R6) to center the trace.